Histol Histopathol (2022) 37: 461-474

**http://www.hh.um.es**

Histology and Histopathology
*From Cell Biology to Tissue Engineering*

**ORIGINAL ARTICLE** **Open Access**

# Lidocaine represses the malignant behavior of lung carcinoma cells via the circ_PDZD8/miR-516b-5p/GOLT1A axis

**Huafen Zi, Li Chen and Qian Ruan**

Department of Anesthesiology, the First Affiliated Hospital of Chengdu Medical College, Sichuan, PR China

**Summary.** Lung carcinoma is the most prevalent malignancy in adults. Lidocaine (Lido) has been confirmed to exert an anti-tumor role in many human cancers. However, the role and underlying mechanism of Lido in lung carcinoma remain poorly understood. Cell proliferation ability, migration, invasion, and apoptosis were measured by Colony formation, 5-ethynyl-2'-deoxyuridine (EdU), Cell Counting Kit-8 (CCK-8), transwell, and flow cytometry assays. Circ_PDZD8, microRNA-516b-5p (miR-516b-5p), and Golgi transport 1A (GOLT1A) levels were detected by real-time quantitative polymerase chain reaction (RT-qPCR). Protein levels of proliferating cell nuclear antigen (PCNA) and GOLT1A were examined by western blot assay. The binding relationship between miR-516b-5p and circ_PDZD8 or GOLT1A was predicted by circular RNA Interactome or Starbase 3.0 and then verified by a dual-luciferase reporter assay. The biological roles of circ_PDZD8 and Lido on lung carcinoma cell growth were examined by the xenograft tumor model in vivo. Lido suppressed proliferation, migration, invasion, and induced apoptosis in lung carcinoma cells. Circ_PDZD8 and GOLT1A were increased, miR-516b-5p was decreased in lung carcinoma tissues and cell lines. Their expression presented the opposite trend in Lido-triggered lung carcinoma cells. Circ_PDZD8 might overturn the repression of Lido on cell growth ability and metastasis in this tumor. Mechanically, circ_PDZD8 might regulate GOLT1A expression by sponging miR-516b-5p. Circ_PDZD8 weakened the anti-lung carcinoma effect of Lido in vivo. Circ_PDZD8 might mitigate the inhibitory effect of Lido on tumor cell malignancy by modulating the miR-516b-5p/GOLT1A axis, providing a novel insight for lung carcinoma treatment.

*Corresponding Author:* Qian Ruan, 278 Baoguang Dadao, Xindu District, Chengdu City, Sichuan Province, China. e-mail: rq881231@163.com

DOI: 10.14670/HH-18-423

**Key words:** Circ_PDZD8, miR-516b-5p, GOLT1A, Lung carcinoma, Lidocaine

## Introduction

Lung carcinoma remains the most prevalent lethal malignancy which threatens public health continuously all over the world (Bray et al., 2018). According to the United States cancer statistics, 235760 new cases of lung carcinoma occurred in 2021 and resulted in 131,880 deaths (Siegel et al., 2021). Regardless of recent considerable advances in comprehensive treatment, including surgical resection and adjuvant chemo-radiotherapy, the majority of patients are diagnosed at an advanced stage with a poor prognosis (Jones and Baldwin, 2018). Thus, sustained attention and research on more effective therapies are urgent and of clinical significance for the disease. At present, the local anesthetic and antiarrhythmic properties of Lidocaine (Lido) have drawn great attention in human disease therapeutics (Lev and Rosen, 1994; Pleguezuelos-Villa, et al., 2019). Due to the salient features of Lido, such as fast onset, a broad range of safety, and good ability to permeate mucosa, the application of Lido in treating diverse diseases has been widely understood (Ko et al., 2007; Mitchell et al., 2009; Sisti et al., 2019). Notably, further studies exhibited that Lido and other local anesthetics have powerful anti-tumor properties in multiple cancers (Liu et al. 2020), including lung carcinoma (Piegeler et al., 2012). However, the mechanism of Lido on lung carcinoma progression is far from clear.

During the past decades, a large number of scholars have discovered that the human genome is pervasively transcribed and produces non-coding RNAs, which present an important role in a wide variety of biological processes (Consortium et al., 2007; Hombach and Kretz, 2016). As a naturally-occurring family of non-coding RNAs, circular RNAs (circRNAs) consists of a closed circular structure, most of which is mainly produced by

the unique back splicing mechanism (Belousova et al., 2018; Kristensen et al., 2019). In addition, they are abundant, conserved, stable, and have tissue- and development-specific expression patterns, highlighting the latent biomarkers for human diseases, including cancer (Ng et al., 2018; Patop and Kadener, 2018). Work in a number of laboratories has revealed that the aberrant expression of circRNAs was inextricably associated with the development of lung carcinoma (Braicu et al., 2019; Wang et al., 2020a,b). For example, Chen et al. found that the highly expressed circRNA 100146 might intensify the malignant phenotype of lung carcinoma by accelerating cell proliferation and invasion in vitro (Chen et al., 2019). Meanwhile, Chi et al. presented that circPIP5K1A might function as an oncogene through direct interaction with the miR-600/HIF-1α axis (Chi et al., 2019). Lately, a well-known circRNA correlated with lung carcinoma, circ_PDZD8 (also named hsa_circ_0020123) has been identified as a potential attractive biomarker, and exerts oncogenic properties by regulating cell growth and metastasis in lung carcinoma (Wan et al., 2019; Bi et al., 2020). Intriguingly, an extensive body of recent research has been reported that the anticancer activity of Lido might be implicated with the regulation of circRNAs in many cancers, such as colorectal cancer, hepatocellular carcinoma, and glioma (Du et al., 2020; Wen et al., 2021; Zhao et al., 2021). Nevertheless, the precise roles played by the expressed circ_PDZD8 in Lido-associated lung carcinoma development remain unclear.

Up to now, increasing evidence has shown that the circRNAs-microRNAs (miRNAs)-mRNAs regulatory mechanism in tumor research is a rapidly expanding field (Cai et al., 2020; Xu et al., 2020). As stable transcripts with a host of miRNA-binding sites, circRNAs were able to act as the competing endogenous RNAs (ceRNAs) to sequester miRNAs away from their target gene (Hansen et al., 2013; Panda, 2018). In the present review, bioinformatics analysis displayed that circ_PDZD8 is able to share some binding sites with miR-516b-5p. Furthermore, miR-516b-5p has been recently proved to be the tumor-suppressive function in esophageal squamous cell carcinoma and endometrial cancer (Zhao et al., 2018; Yang et al., 2020). Synchronously, relevant studies suggested that abnormal expression of miR-516b-5p might suppress cell growth ability and metastasis of lung carcinoma (Zhu et al., 2017; Song et al., 2020). Hence, this study is designed to preliminarily investigate whether the regulatory role of circ_PDZD8 in Lido-caused anti-lung carcinoma activity was mediated by sponging miR-516b-5p.

## Materials and methods

### *Cell culture and treatment*

Lung carcinoma cell lines (A549: RCB0098, PC9: RCB4455; Riken BRC, Tuskuba, Japan) were respectively cultured in DMEM medium (PAN Biotech, Aidenbach, Germany) and RPMI1640 medium (Sigma-Aldrich, St. Louis, MO, USA), followed by addition with 10% fetal bovine serum (FBS; Hyclone, Logan, UT, USA) and 1% penicillin/streptomycin (PAN Biotech). Also, normal human bronchial epithelial cells (HBE: CL-0346, Procell, Wuhan, China) were grown routinely in a special medium (CM-0346, Procell). All cells were maintained in a humidified atmosphere containing 5% $CO_2$ at 37°C, followed by treatment with different dosages of Lido (Sigma-Aldrich) for 48 h. In addition, to evaluate the stability of circ_PDZD8, A549 and PC9 cells were incubated with Actinomycin D (2 mg/mL, Sigma-Aldrich) for 0, 8, 16, and 24 h at 37°C.

### *Colony formation assay*

Un-transfected or transfected A549 and PC9 cells were placed in 6-well culture plates, followed by exposure to Lido for 48 h. After an incubation period of 14 days, treated cells were stained with 0.1% crystal violet solution after being mixed with 4% formaldehyde. 30 min later, different groups were subjected to microscopic analysis.

### *5-ethynyl-2'-deoxyuridine (EdU) assay*

In 6-well plates, $5\times10^4$ treated tumor cells were incubated in the culture medium for 24 h. After being mixed with EdU (50 μM, RiboBio, Guangzhou, China) for 2 h, cells were fixed in 4% formaldehyde before being mixed with Apollo Dye Solution and DAPI (identifying the nuclei). After incubation for 30 min, the stained cells were assessed by fluorescence microscope.

### *Cell Counting Kit (CCK-8) assay*

In short, $5\times10^3$ treated cells were seeded into each well of 96-well culture plates, followed by incubation for 24 h. After mixture with 10 μL of CCK-8 reagents (Dojindo, Kumamoto, Japan) for 2 h, the absorbance at 450 nm was observed by means of a microplate reader (Bio-Rad, Hercules, CA, USA) at different time points.

### *Transwell assay*

In general, treated tumor cells were re-suspended in a serum-free medium, followed by introduction into the upper chamber (BD Biosciences, Heidelberg, Germany). Meanwhile, the bottom chamber housed the medium containing 10% FBS. After 24 h of incubation, 0.1% crystal violet (Sigma-Aldrich) was added to each well for staining the cells that migrated through the bottom side. , The stained cells were then counted under a microscope (magnification ×100). For invasion assay, the same steps as for the migration assay were followed, except that the inserts were pre-coated with Matrigel (BD Bioscience).

### *Cell apoptosis assay*

In brief, treated tumor cells in 6-well plates were

trypsinized and washed, followed by re-suspension in binding buffer (Bender Med System, Vienna, Austria). Then, 5 μL of equal amounts of Annexin V-FITC and PI (Bender Med System) was added into each well and put in the dark. After being incubated for 15 min, different groups were analyzed according to the user's guidebook of a FACSCalibur (Becton Dickinson, Franklin Lakes, NJ, USA).

### *Real-time quantitative polymerase chain reaction (RT-qPCR)*

Whole-RNA from lung carcinoma cell lines was prepared using the standard procedure of Trizol reagent (Invitrogen), followed by quantification with a NanoDrip spectrophotometer (NanoDrop Technologies, Wilmington, DE, USA). After synthesizing template DNA using Prime Script RT Master Mix (TaKaRa, Dalian, China), amplification reaction was carried out using SYBR Green Master Mix (Invitrogen) and the specific primers. After normalization to GAPDH or U6, the obtained data were analyzed according to the $2^{-\Delta\Delta Ct}$ method. Primers were presented as follows:

Circ_PDZD8: 5'-GTATGCACTCTGGCCTGCTT-3' (sense), 5'-ACCCATCAGTTGACTGGACA-3' (antisense); Linear PDZD8 mRNA: 5'-ACTAGTTTG GGCTGGTTTTGTT-3' (sense), 5'-ACAACTGTAAG ACGCCAAAGC-3' (antisense); miR-516b-5p: 5'-GCG CGATCTGGAGGTAAGAAG-3' (sense), 5'-AGTGCA GGGTCCGAGGTATT-3' (antisense); GOLT1A: 5'-ACGGCACAAACTCAAGGGAACC-3' (sense), 5'-AGACATTGCCCAGGAAGCCGAA-3' (antisense); U6: 5'-CTCGCTTCGGCAGCACA-3' (sense), 5'-AAC GCTTCACGAATTTGCGT-3' (antisense); GAPDH: 5'-GGTCACCAGGGCTGCTTT-3' (sense), 5'-GGAAGAT GGTGATGGGATT-3' (antisense).

### *Subcellular fractionation assay*

In this assay, PARIS kit (Ambion, Austin, TX, USA) was used to analyze the subcellular localization of circ_PDZD8. Generally, collected tumor cells were resuspended into cell fractionation buffer. Thereafter, the cytoplasmic supernatant was aspirated away from the nuclear pellet, which was lysed in the nucleus lysis buffer. After the extraction of the cytoplasmic and nuclear RNA, RT-qPCR assay was performed to assess circ_PDZD8 expression in both fractions.

### *Cell transfection*

To stable express circ_PDZD8, tumor cells at 50% confluence were infected with vector or circ_PDZD8 (Geneseed, Shanghai, China) by virus particles in media including8 μg/mL of polybrene (Sigma-Aldrich). One day later, the vector-positive cells were selected using puromycin. Meanwhile, $2\times10^5$ tumor cells were transfected with 20 nM of the oligonucleotides, containing miR-516b-5p mimic, inhibitor, GOLT1A small interference RNA (si-GOLT1A), and their controls (miR-NC, anti-miR-NC, si-NC), according to the supplier's direction of Lipofectamine 3000 (Invitrogen).

### *Western blot assay*

After being lysed using RIPA lysis buffer (Beyotime, Shanghai, China), the cell lysates were subjected to 10% separating gel and then shifted to nitrocellulose membranes (Millipore, Molsheim, France). Subsequently, the primary antibodies: proliferating cell nuclear antigen (PCNA, 1:1000, ab92552, Abcam, Cambridge, MA, USA), GOLT1A (1:1000, ab272565, Abcam), GAPDH (ab8227, 1:1000), and the secondary antibody were probed onto the membranes. Finally, the proteins were visualized by means of ECL reagent (Millipore).

### *Dual-luciferase reporter assay*

The binding between miR-516b-5p and circ_PDZD8 or GOLT1A was analyzed using the bioinformatics software circular RNA Interactome (https://circinteractome.nia.nih.gov) and Starbase 3.0 (http://starbase.sysu.edu.cn). Thereafter, in dual-luciferase reporter assay, the wild-type (WT) luciferase reporter constructs (circ_PDZD8-WT or GOLT1A 3'UTR-WT) containing miR-516b-5p-specific binding sites and the site-directed mutant (MUT) constructs (circ_PDZD8-MUT or GOLT1A 3'UTR-MUT) were provided by Hanbio (Shanghai, China). Then, A549 and PC9 cells were co-transfected with the constructs with miR-516b-5p or miR-NC, followed by analysis by a dual-luciferase reporter assay system (Promega, Madison, WI, USA).

### *Tumor xenograft assay*

Twenty male BALB/C nude mice (Vital River Laboratory, Beijing, China) were used in this animal experiment, which was conducted following the Animal Ethics Committee of the First Affiliated Hospital of Chengdu Medical College. Five-week-old mice were arranged into 4 groups (Control, Lido, Lido + Vector, and Lido + circ_PDZD8) with 5 mice in each group, followed by subcutaneous inoculation using A549 cells ($2\times10^6$) with or without vector and circ_PDZD8. 10 days later, these mice were administrated with lidocaine (1.5 mg/kg) via tail vein injection or PBS every 5 days. Meanwhile, tumor volume was detected and calculated every 5 days. After a month, all mice were killed and tumor masses were weighed and imaged. Also, immunohistochemical staining was performed according to the prior description (Jiang, et al. 2016), with antibodies specific for GOLT1A and Ki-67 to assess proliferation.

### *Statistical analysis*

GraphPad Prism7 (GraphPad Prism software, San

Diego, CA, USA) was used to analyze all results, which are given as the mean ± standard deviation (SD) with statistical significance suggested when $P<0.05$. The comparisons between groups were performed based on Student's t-test or one-way analysis of variance (ANOVA) with Tukey's tests.

## Results

### *Lido might hinder cell growth ability and metastasis in lung carcinoma*

Firstly, to investigate the biological function of Lido in Lung carcinoma, A549 and PC9 cells were treated with different concentrations of Lido for 24 h. Subsequently, Colony formation assay and EdU assay suggested that colony number and EdU-positive cells were gradually reduced in A549 and PC9 cells after treatment with 4 mM and 8 mM Lido (Fig. 1A,B). Also, CCK-8 results displayed that Lido treatment also might decrease A549 and PC9 cell viability in a certain concentration-dependent manner (Fig. 1C,D). Apart from that, transwell assays displayed that the abilities of migration and invasion of A549 and PC9 cells were repressed with the increase of Lido concentration (Fig. 1E,F). By contrast, an overt enhancement of apoptosis rate was observed due to the treatment of Lido in A549 and PC9 cells (Fig. 1G). In short, Lido was able to

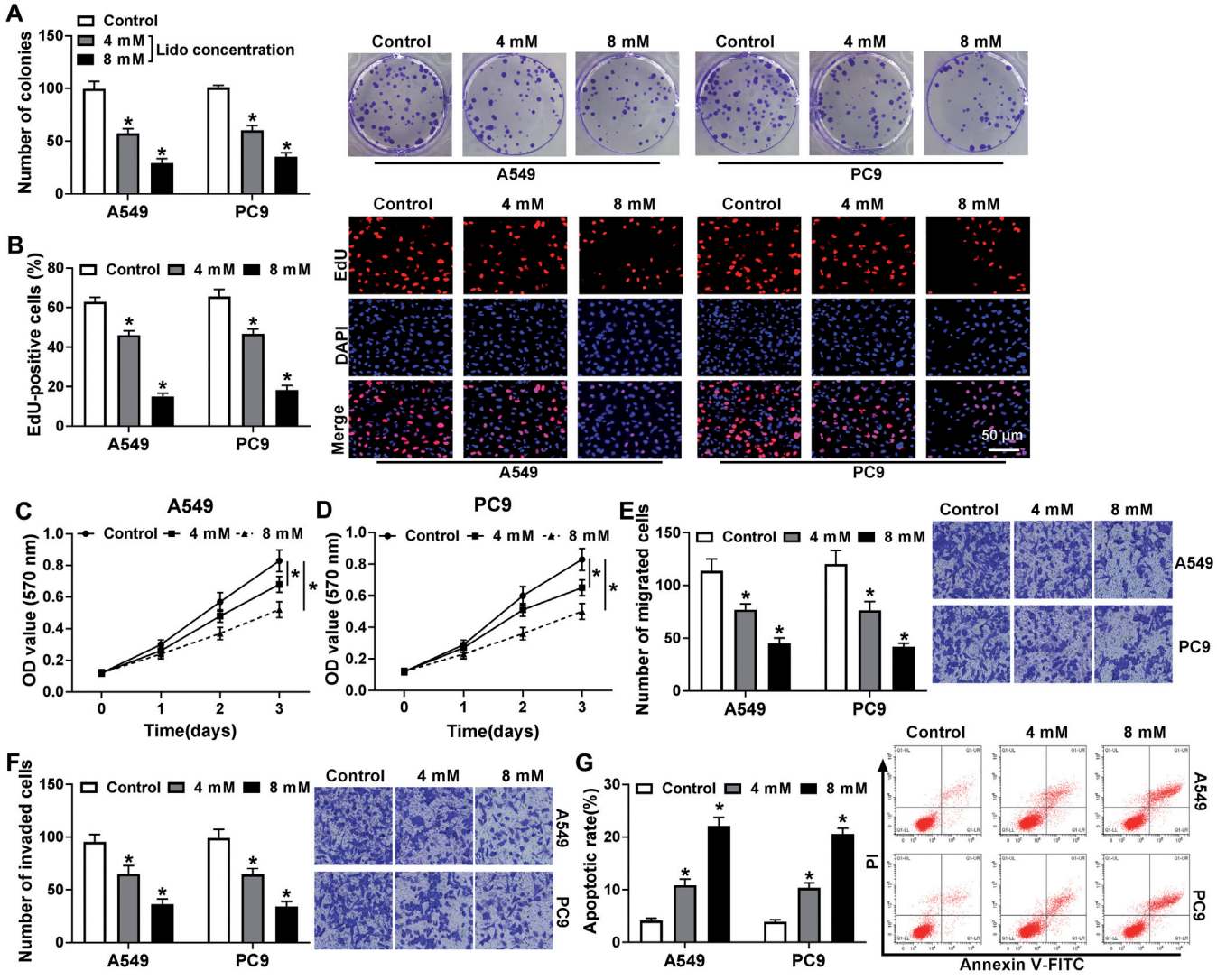


**Fig. 1.** The effect of Lido on the malignant phenotype in lung carcinoma cells. A549 and PC9 cells were stimulated with Control, 4 mM Lido, and 8 mM Lido. **A.** Colony formation assay for colony number was assessed in treated A549 and PC9 cells. **B.** EdU assay for EdU-positive cells was measured in treated A549 and PC9 cells. **C, D.** CCK-8 assay for cell viability was examined in treated A549 and PC9 cells. **E, F.** Transwell assays for migration and invasion were detected in treated A549 and PC9 cells. **G.** Flow cytometry assay for apoptosis rate was analyzed in treated A549 and PC9 cells. *$P<0.05$.

inhibit cell growth ability and metastasis of lung carcinoma cells in a dose-dependent manner. Also, since with Lido at the concentration of 8 mM for 24 h the suppressing effects achieved the most, 8 mM Lido treatment for 24 h was selected for the following experiments.

### *Circ_PDZD8 expression was decreased in Lido-treated lung carcinoma cells*

Of interest, we found that Lido exposure was able to reduce the expression level of circ_PDZD8 in A549 and PC9 cells (Fig. 2A), implying that circ_PDZD8 downregulation induced by Lido might be involved with the anti-tumor properties of Lido in lung carcinoma. Meanwhile, RT-qPCR assay exhibited that circ_PDZD8 level was upregulated in A549 and PC9 cells compared with normal human bronchial epithelial (HBE) cells (Fig. 2B), suggesting the underlying carcinogenic role of circ_PDZD8 in lung carcinoma. Then, to validate the circular characteristics of circ_PDZD8, A549 and PC9 cells treated with Actinomycin D. As shown in Fig. 2C,D, the half-life of circ_PDZD8 transcript exceeded 24 h, manifesting that this isoform is more stable than the linear PDZD8 mRNA transcript in A549 and PC9 cells. Besides, subcellular fractionation assay displayed that circ_PDZD8 was predominantly located in the cytoplasm of A549 and PC9 cells (Fig. 2E,F), indicating the potential post-transcriptional regulatory mechanism of circ_PDZD8 in lung carcinoma cells.

### *Upregulation of circ_PDZD8 might attenuate Lido triggered inhibition of lung carcinoma*

Next, to explore the influence of circ_PDZD8 on Lido-induced malignant phenotype inhibition of lung carcinoma cells, circ_PDZD8 was transfected into A549 and PC9 cells before Lido treatment. Data suggested that circ_PDZD8 expression, rather than PDZD8 mRNA, was markedly increased in A549 and PC9 cells (Fig. 3A,B). Thereafter, the Colony formation assay and EdU assay presented that the overexpression of circ_PDZD8 was able to remarkably reduce the negative effect of Lido on cell proliferation in A549 and PC9 cells (Fig. 3C,D). Consistently, the introduction of circ_PDZD8 also was able to abate the Lido-caused decrease in cell viability in A549 and PC9 cells (Fig. 3E,F). Synchronously, to further verify the effect of circ_PDZD8 and Lido on cell proliferation ability, PCNA expression (a proliferation marker) was determined in A549 and PC9 cells. As displayed in Fig. 3G, the treatment of Lido elicited an obvious decline in PCNA protein level in A549 and PC9 cells, whereas circ_PDZD8 upregulation was able to distinctly overturn

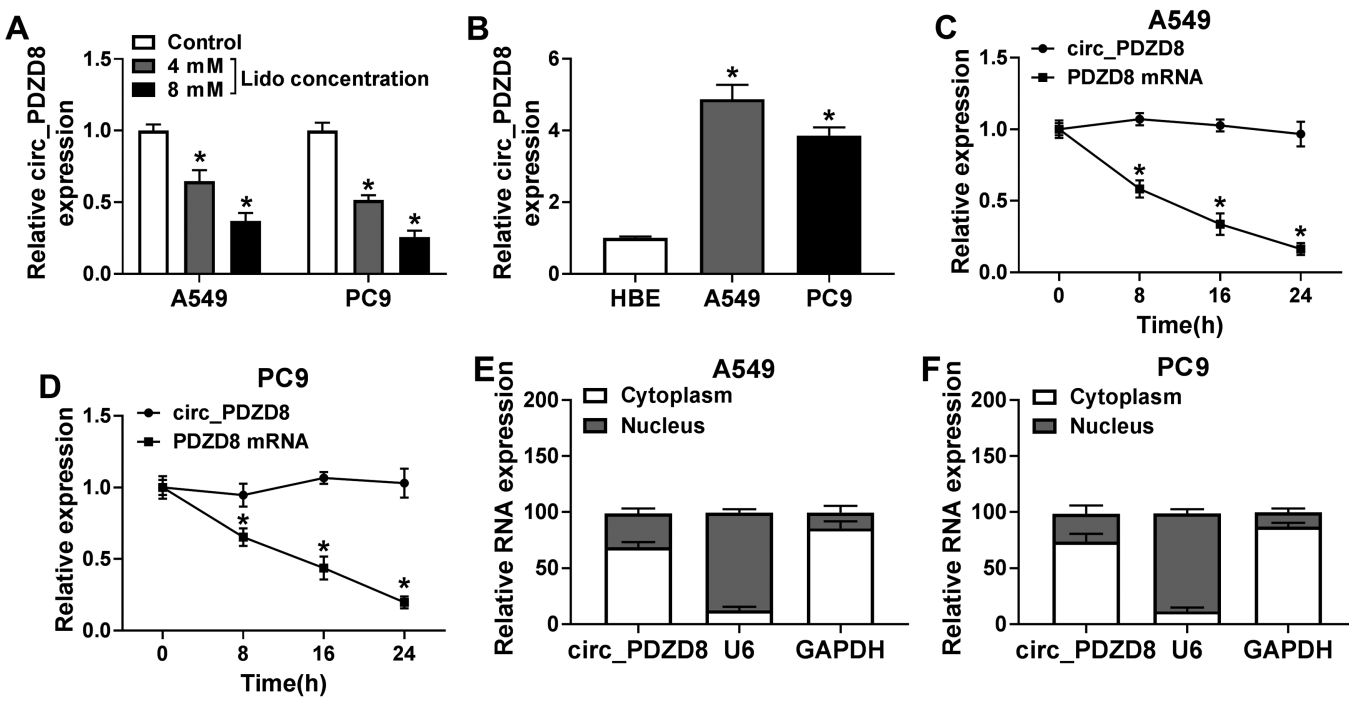


**Fig. 2.** Lido reduced circ_PDZD8 expression in lung carcinoma cells. **A.** RT-qPCR analysis of circ_PDZD8 expression in A549 and PC9 cells treated with Control, 4 mM Lido, and 8 mM Lido. **B.** Circ_PDZD8 level was determined in HBE, A549, and PC9 cells by RT-qPCR assays. **C, D.** Relative levels of circ_PDZD8 and PDZD8 mRNA were detected by RT-qPCR assay in A549 and PC9 cells treated with Actinomycin D. **E, F.** The cellular localization of circ_PDZD8 in A549 and PC9 cells was analyzed by Subcellular fractionation assay. *P<0.05.

the effect. Moreover, transwell assays exhibited that the suppression of migration and invasion caused by Lido was partly weakened by elevated circ_PDZD8 in A549 and PC9 cells (Fig. 3H,I). In addition, flow cytometry assay showed that Lido-triggered improvement in apoptosis rate was also partially abrogated in A549 and PC9 cells after circ_PDZD8 transfection (Fig. 3J). Collectively, these results suggested that Lido might

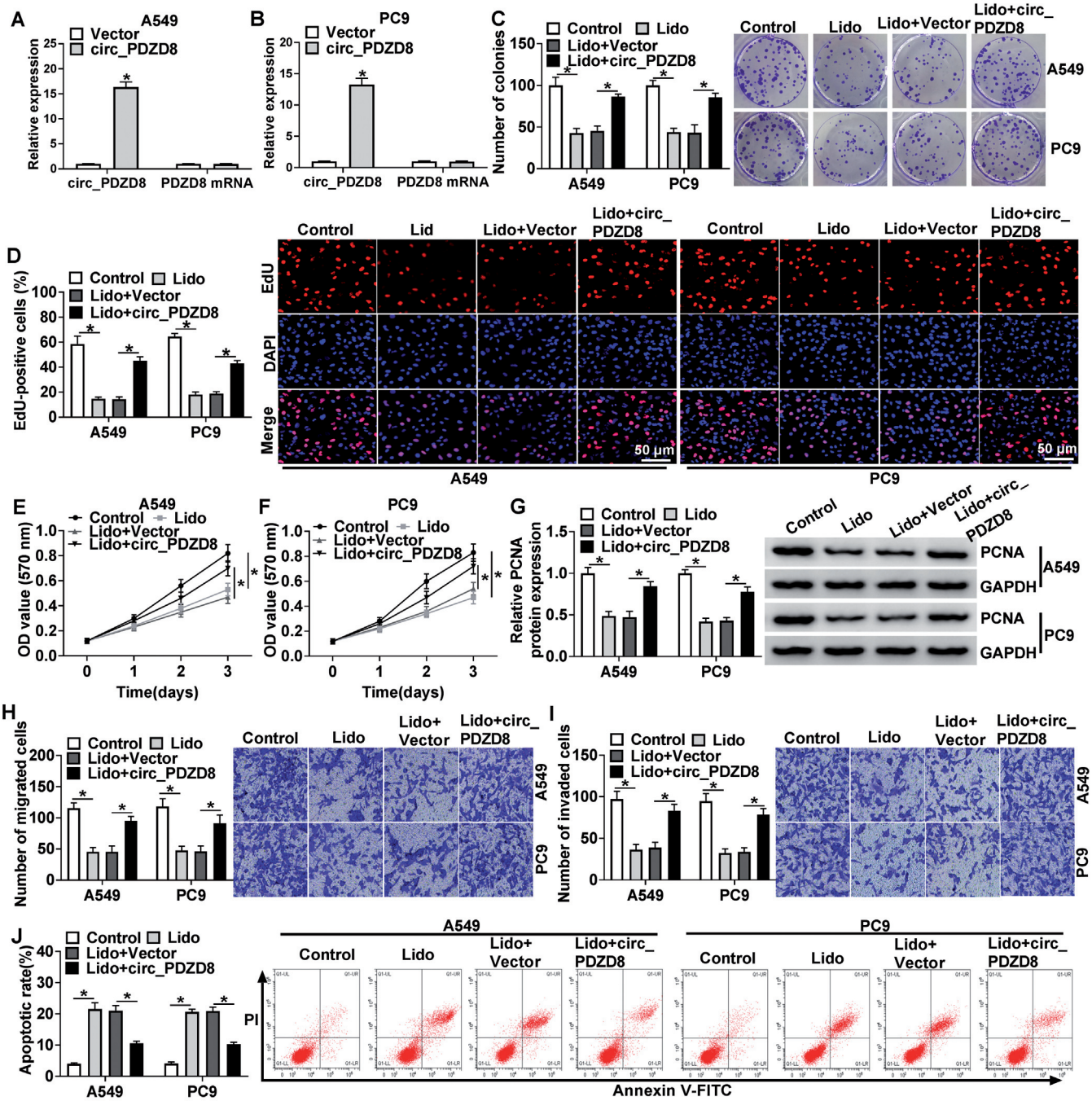


**Fig. 3.** The effect of circ_PDZD8 on Lido-mediated suppression in cell growth and metastasis in lung carcinoma cells. **A, B.** RT-qPCR analysis of circ_PDZD8 and PDZD8 mRNA expression in A549 and PC9 cells. (C-J) A549 and PC9 cells were treated with Control, Lido, Lido + vector, and Lido + circ_PDZD8. **C, D.** Cell proliferation was detected in treated A549 and PC9 cells by Colony formation assay and EdU assay. **E, F.** Cell viability was measured in treated A549 and PC9 cells by CCK-8 assay. **G.** Western blot analysis of PCNA expression in treated A549 and PC9 cells. **H, I.** Migration and invasion were examined in treated A549 and PC9 cells by transwell assay. **J.** Apoptosis rate was assessed in treated A549 and PC9 cells by flow cytometry assay. *P<0.05.

block lung carcinoma development by regulating circ_PDZD8.

*Circ_PDZD8 was a sponge of miR-516b-5p*

To further discover the possible mechanism by which circ_PDZD8 functioned, we searched putative circ_PDZD8-interacting miRNAs using the bioinformatics software circular RNA Interactome. As shown in Fig. 4A, miR-516b-5p was predicted as a candidate target of circ_PDZD8, and the predicted binding sites were also presented. To confirm the interaction of miR-516b-5p with circ_PDZD8 was mediated by the putative binding site, a dual-luciferase reporter assay was conducted. Results suggested that the luciferase activity of report vectors carrying circ_PDZD8-WT was evidently reduced by miR-516b-5p upregulation in A549 and PC9 cells, while vectors equipped with circ_PDZD8-MUT exhibited little change in the luciferase activity in cells transfected with miR-516b-5p or miR-NC (Fig. 4B,C). Simultaneously, we noticed that the miR-516b-5p level was greatly decreased by the overexpression of circ_PDZD8 in A549 and PC9 cells (Fig. 4D). Interestingly, RT-qPCR indicated that the treatment of Lido might block the expression level of miR-516b-5p in A549 and PC9 cells (Fig. 4E), implying the involvement of miR-516b-5p in Lido-mediated lung carcinoma progression. Additionally, the significant downregulation of miR-516b-5p was viewed in A549 and PC9 cells relative to the normal human bronchial epithelial (HBE) cells (Fig. 4F). Together, these data suggested that circ_PDZD8 regulated the abundance of miR-516b-5p via binding to miR-516b-5p.

*Circ_PDZD8 might attenuate the anti-tumor activity of Lido by interacting with miR-516b-5p in lung carcinoma cells*

In view of the regulatory role of circ_PDZD8 in miR-516b-5p expression in A549 and PC9 cells, we further investigated whether the impact of circ_PDZD8 on Lido-mediated regulation of lung carcinoma malignancy was related to miR-516b-5p. At first, RT-qPCR assay displayed that the forced expression of circ_PDZD8 was obviously able to reduce the expression level of miR-516b-5p in A549 and PC9 cells, which was partly counteracted by miR-516b-5p mimic (Fig. 5A). Functionally, we observed that cell proliferation ability improved by circ_PDZD8 upregulation was partly undermined via miR-516b-5p mimic in Lido-induced A549 and PC9 cells (Fig. 5B-5E), as evidenced by declined PCNA level (Fig. 5F). Concurrently, transwell assays exhibited that the upregulation of miR-516b-5p was able to reverse the migration and invasion-promotion effect of circ_PDZD8 in Lido-treated tumor cells (Fig. 5G,H). Besides, the inhibitory of cell apoptosis rate caused by circ_PDZD8 elevated was distinctly abrogated by miR-516b-5p overexpression in Lido-triggered tumor cells (Fig. 5I). Taken together, Circ_PDZD8 was able to relieve Lido-caused lung carcinoma cell growth ability loss, metastasis decrease, and apoptosis induction by sponging miR-516b-5p in vitro.

*GOLT1A was a target of miR-516b-5p*

Subsequently, bioinformatics analysis (Starbase 3.0)

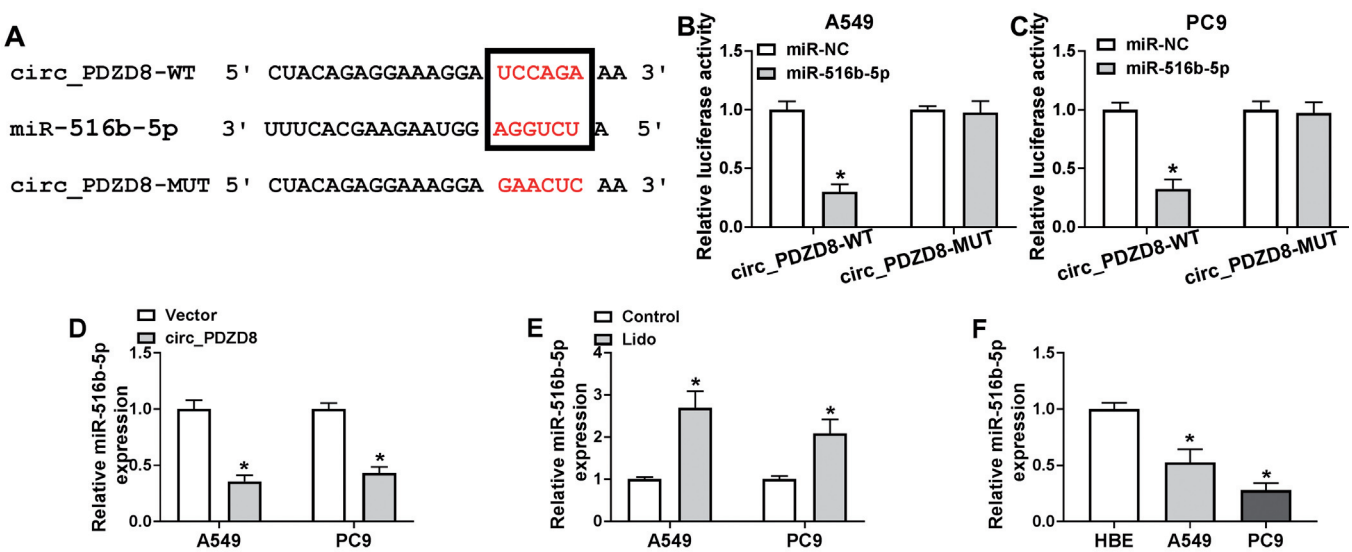


**Fig. 4.** Circ_PDZD8 was able to target regulating miR-516b-5p. **A.** Schematic of a putative target sequence for miR-516b-5p in circ_PDZD8 and mutated miR-516b-5p-binding sites. **B, C.** The binding relationship was verified by a dual-luciferase reporter assay. **D.** RT-qPCR analysis of miR-516b-5p expression in vector or circ_PDZD8-transfected A549 and PC9 cells. **E.** miR-516b-5p level was determined in control or Lido-treated A549 and PC9 cells by RT-qPCR assay. **F.** miR-516b-5p level examined in HBE, A549, and PC9 cells by RT-qPCR assays. *P<0.05.

was applied to explore the putative targets of miR-516b-5p, and GOLT1A as one candidate with the predicted binding sites on miR-516b-5p was exhibited in Fig. 6A. Then, a dual-luciferase reporter assay presented that miR-516b-5p upregulation led to a striking decline in the luciferase activity of GOLT1A 3'UTR-WT reporter vector but not that of GOLT1A 3'UTR-MUT reporter vector (Fig. 6B,C). To verify the actual effect of miR-516b-5p on GOLT1A in tumor cells, miR-516b-5p mimic or anti-miR-516b-5p was synthesized and introduced into A549 and PC9 cells, followed by the detection of transfection efficiency (Fig. 6D). After that, RT-qPCR assay and western blot assay displayed that the upregulation of miR-516b-5p was able to hinder GOLT1A expression level, while miR-516b-5p downregulation might boost GOLT1A level in A549 and PC9 cells (Fig. 6E,F). Also, the significant upregulation of GOLT1A was found in lung carcinoma cell lines in comparison with the control group (Fig. 6G,H). Of note, we viewed that the treatment of Lido might restrain the expression level of GOLT1A in tumor cells (Fig. 6I,J), suggesting that the dysregulation of GOLT1A might be associated with Lido-mediated tumor progression. Interestingly, our results exhibited that the overexpression of circ_PDZD8 was able to enhance GOLT1A expression level, and the co-transfection of miR-516b-5p mimic partially abolished the effect in A549 and PC9 cells (Fig. 6K,L), indicated that circ_PDZD8 might act as a sponge of miR-516b-5p to affect GOLT1A expression. Overall, these data

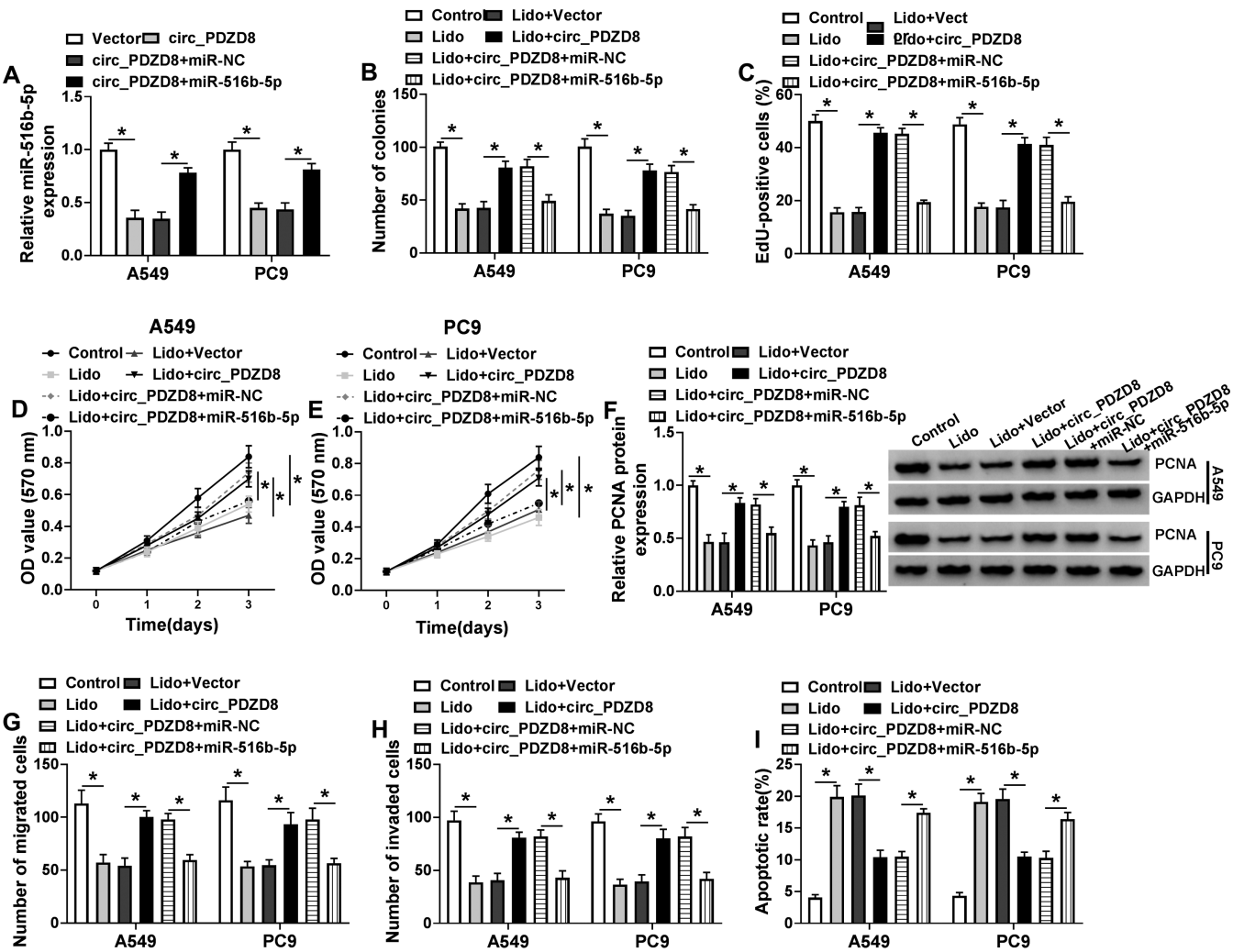


**Fig. 5.** Lido exerted anti-tumor activity by regulating the circ_PDZD8/miR-516b-5p axis in lung carcinoma cells. **A.** miR-516b-5p level was determined by RT-qPCR assay in A549 and PC9 cells transfected with Vector, circ_PDZD8, circ_PDZD8 + miR-NC, and circ_PDZD8 + miR-516b-5p. **B-I.** Transfected A549 and PC9 cells were treated with Lido. **B, C.** Colony formation assay and EdU assay were used to detect cell proliferation in treated A549 and PC9 cells. **D, E.** CCK-8 assay was applied to assess cell viability in treated A549 and PC9 cells. **F.** Western blot was performed to determine the protein level of PCNA in treated A549 and PC9 cells. **G, H.** Transwell assays were implemented to analyze migration and invasion in treated A549 and PC9 cells. **I.** Flow cytometry assay was carried out to examine apoptosis rate in treated A549 and PC9 cells. *P<0.05.

discovered that GOLT1A was a direct target of miR-516b-5p.

### *miR-516b-5p knockdown attenuated Lido-caused malignant progression by regulating GOLT1A in lung carcinoma cells*

Subsequently, we conducted rescue assays to ascertain that the effects of miR-516b-5p on Lido-triggered inhibition of lung carcinoma cell malignant behaviors were related to GOLT1A. As shown in Fig. 7A,B, the re-introduction of si-GOLT1A was able to abolish the anti-miR-516b-5p-caused increase in GOLT1A expression in A549 and PC9 cells. Then, functional analysis suggested that miR-516b-5p knockdown-induced cell growth ability elevation was distinctly weakened by GOLT1A downregulation in both Lido-treated A549 and PC9 cells (Fig. 7C-F), which was accompanied by the reduction of PCNA level (Fig. 7G). Apart from that, the promotion role of migration and

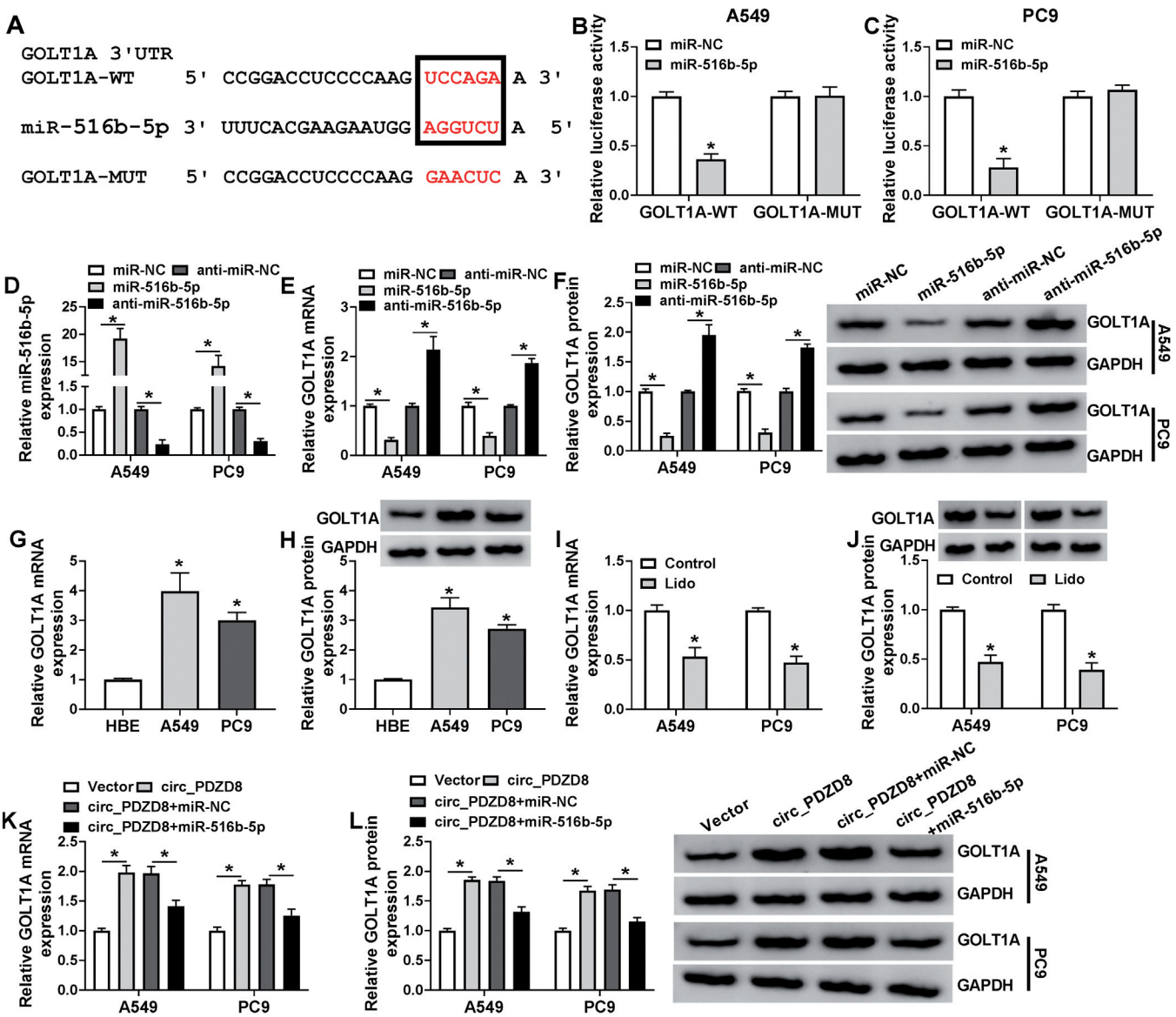


**Fig. 6.** miR-516b-5p was able to directly target GOLT1A. **A.** The predicted binding sites between miR-516b-5p and the 3'UTR of GOLT1A. **B, C.** A dual-luciferase reporter assay was used to verify the binding. **D.** RT-qPCR analysis of miR-516b-5p expression in A549 and PC9 cells transfected with miR-NC, miR-516b-5p, anti-miR-NC, and anti-miR-516b-5p. **E, F.** The effects of miR-516b-5p upregulation or downregulation on GOLT1A expression were detected by RT-qPCR assay or western blot assay. **G, H.** GOLT1A expression was determined in HBE, A549, and PC9 cells. **I, J.** RT-qPCR assay or western blot analysis of GOLT1A level in A549 and PC9 cells treated with or without Lido. **K, L.** GOLT1A expression was determined in A549 and PC9 cells transfected with Vector, circ_PDZD8, circ_PDZD8 + miR-NC, and circ_PDZD8 + miR-516b-5p.*P<0.05.

invasion caused by miR-516b-5p inhibitor also was overturned by deficiency of GOLT1A in Lido-exposed A549 and PC9 cells (Fig. 7H,I). Additionally, flow cytometry results indicated that the silencing of GOLT1A might partly abrogate anti-miR-516b-5p-mediated apoptosis loss in Lido-treated A549 and PC9 cells (Fig. 7J). All of these data implied that miR-516b-5p was able to regulate cell malignant behaviors in Lido-

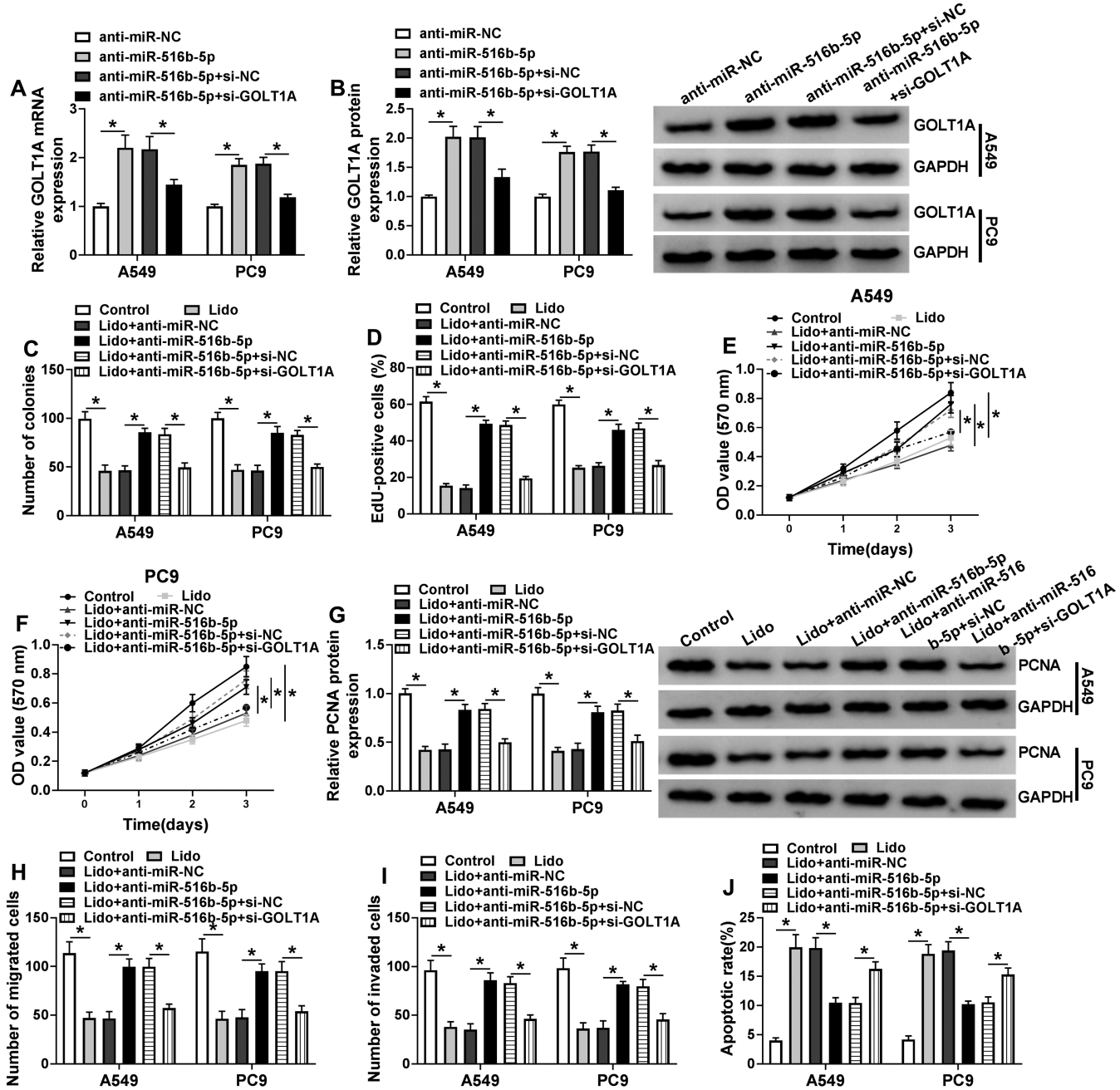


**Fig. 7.** The effects of miR-516b-5p knockdown on malignant progression were overturned by regulating GOLT1A in Lido-treated lung carcinoma cells. **A, B.** RT-qPCR assay or western blot analysis of GOLT1A level in A549 and PC9 cells transfected with anti-miR-NC, anti-miR-516b-5p, anti-miR-516b-5p + si-NC, and anti-miR-516b-5p + si-GOLT1A. (C-J) Transfected tumor cells were treated with Lido. **C, D.** The detection of cell proliferation was performed using Colony formation assay and EdU assay in treated A549 and PC9 cells. **E, F.** The measurement of cell viability was conducted using CCK-8 assay in treated A549 and PC9 cells. **G.** The determination of PCNA protein level was carried out using western blot assay in treated A549 and PC9 cells. **H, I.** The assessment of migration and invasion was implemented using transwell assay in treated A549 and PC9 cells. **J.** The analysis of apoptosis rate was executed using flow cytometry assay in treated A549 and PC9 cells. *P<0.05.

treated lung carcinoma by targeting GOLT1A.

*Lido was able to repress cell growth of lung carcinoma by regulating circ_PDZD8 in vivo*

Additionally, mice xenograft models of lung carcinoma were established to investigate the effect of circ_PDZD8 and Lido on tumor growth. As illustrated in Fig. 8A,B, tumor size and weight dropped in the presence of Lido treatment, while the introduction of circ_PDZD8 might partly mitigate these effects in xenograft. Meanwhile, our results exhibited that stable overexpression of circ_PDZD8 was able to abolish the suppression action of Lido on circ_PDZD8 (Fig. 8C), and GOLT1A levels (Fig. 8E,F) in tumor tissues derived from xenograft. Also, the expression level of miR-516b-5p presented the opposite trend in this xenograft (Fig. 8D). In addition, immunohistochemical staining discovered that Lido-triggered decrease in GOLT1A and Ki-67 (standard proliferation marker) levels, which was overturned by circ_PDZD8 upregulation (Fig. 8G). Thus, it is concluded that Lido was able to dampen lung carcinoma cell growth by modulating circ_PDZD8 in vivo.

## Discussion

Nowadays, a substantial amount of clinical data shows that Lido has received increasing attention for its anesthetic advantages and other pharmacological functions in the treatment of human disease (Beaussier et al., 2018; Soto et al., 2018). In fact, recent evidence has

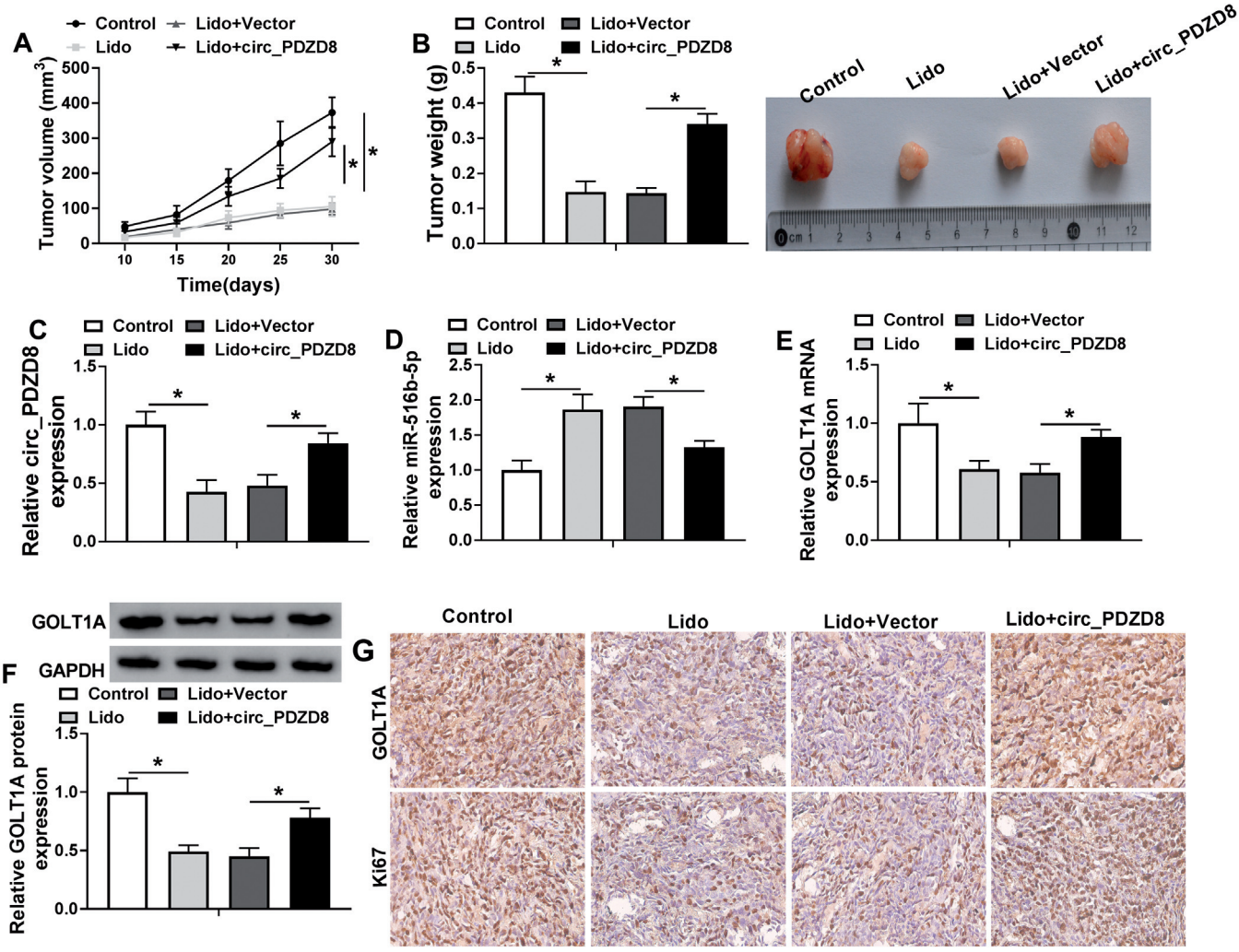


**Fig. 8.** Circ_PDZD8 was able to abrogate the repression of Lido on lung carcinoma cell growth *in vivo*. A549 cells with vector or circ_PDZD8 were inoculated subcutaneously into nude mice, followed by intraperitoneal injection with Lido (1.5 mg/kg) after 10 days. **A, B.** Tumor volume and tumor weight were determined. **C, D.** The levels of circ_PDZD8 and miR-516b-5p were assessed in xenografts by RT-qPCR assay **E, F.** GOLT1A expression level was measured in xenografts by RT-qPCR and western blot assay. **G.** GOLT1A and Ki67 expression were gauged in xenografts by Immunohistochemical staining. *P<0.05.

revealed that Lido is able to perform as a new therapeutic agent to repress the progression of various cancer (D'Agostino et al., 2018; Qu et al., 2018a,b). The current work also confirmed the inhibitory role of Lido on tumor cell growth ability and metastasis in lung carcinoma, coherently with the former reports (Sun and Sun, 2019). Of interest, rapidly accumulating evidence discovered that circRNAs might be involved in the underlying mechanisms by which Lido modulates human cancer development (Guan et al., 2021; Wen et al., 2021). In this paper, our data identified that a typical circRNA, circ_PDZD8 was significantly upregulated in lung carcinoma cell lines, in concordance with a previous study (Qu et al., 2018a,b). Combined with the forementioned findings, we further explored the connection between circ_PDZD8 and Lido. In this research, we are the first to observe that Lido is able to dampen the expression of circ_PDZD8 in the tumor cell lines, suggesting that the anti-tumor role of Lido might be related to circ_PDZD8 expression in this tumor.

Previous literature displayed that uncontrolled proliferation is now considered to be an important contributor to the pathogenesis of solid tumors (Evan and Vousden, 2001; Feitelson et al., 2015). In this article, our data indicated that the upregulation of circ_PDZD8 might relieve Lido-triggered reduction in cell growth ability in two tumor cell lines in vitro. Apart from that, activated metastasis is responsible for the overwhelming cause of the malignancy hallmarks (Zeeshan and Mutahir, 2017; Suhail et al., 2019). The present work manifested that the repression of Lido on migration and invasion was mitigated by circ_PDZD8 elevated in tumor cells. Consistently, xenograft formation assay also revealed that the overexpression of circ_PDZD8 might attenuate Lido-caused decrease in cell growth in vivo. These collective findings indicated that the anti-tumor activity of Lido might be regulated by circ_PDZD8.

Recent reports have described an intricate interplay between circRNAs and miRNAs for post-transcriptional control (Thomas and Saetrom, 2014; Panda, 2018). In this regard, we searched the possible circ_PDZD8-interacting miRNAs using circular RNA Interactome software. Of particular interest, miR-516b-5p was selected as a research object, considering the tumor-suppressor in various cancers. It has been confirmed that the upregulation of miR-516b-5p could hinder cell growth and metastasis in lung carcinoma cells (Zhu et al., 2017; Song et al., 2020). In this paper, our research emphasized that miR-516b-5p was a new miRNA target of circ_PDZD8 for the first time. What's more, the present data displayed that the upregulation of circ_PDZD8 was able to significantly mitigate the anti-tumor activity of Lido in lung carcinoma cells by regulating miR-516b-5p. Additionally, circ_PDZD8 has been confirmed to boost cell growth and metastasis of lung carcinoma by sponging multiple miRNAs (Wang et al., 2020a,b; Ma et al., 2021). These collective findings manifested that circ_PDZD8 might be involved in complex regulatory networks of lung carcinoma progression. Likewise, Starbase 3.0 software analysis suggested that GOLT1A, a transporter on the Golgi membrane (Conchon et al., 1999), appeared to be a strong candidate target for miR-516b-5p. Further studies suggested the knockdown of GOLT1A was able to restrain tumor cell growth and metastasis in breast cancer and adenoid cystic carcinomas (Ikeda et al., 2015; Zhang et al., 2020). Simultaneously, the dysregulation of GOLT1A was related to the anti-proliferation role of Lido in lung carcinoma cells (Zhang et al., 2017). In this study, our results indicated that the silencing of GOLT1A might abolish miR-516b-5p downregulation-mediated increase in malignant behavior in Lido-treated lung carcinoma cells. More importantly, our data proved that the co-transfection of miR-516b-5p was able to, at least partially, overturn the promotion of circ_PDZD8 on GOLT1A expression in lung carcinoma cells, supporting the regulatory role of the circ_PDZD8/miR-516b-5p/GOLT1A axis in lung carcinoma. However, there are still some shortcomings in this research. For example, these data exhibited are according to a limited number of cell or animal assays, and the role of Lido and circ_PDZD8 in healthy cell lines should be detected before the application to clinical use to ensure safety and efficiency.

### *Conclusions*

In summary, these findings discovered that circ_PDZD8 can relieve the anti-cancer activity of Lido partly via the miR-516b-5p/GOLT1A axis. This study elucidates the new mechanism of Lido and sheds light on developing new therapies for lung carcinoma.

*Acknowledgements.* None
*Disclosure of interest.* The authors declare that they have no conflicts of interest.
*Funding.* None.

## References

Beaussier M., Delbos A., Maurice-Szamburski A., Ecoffey C. and Mercadal L. (2018). Perioperative use of intravenous lidocaine. Drugs 78, 1229-1246.

Belousova E.A., Filipenko M.L. and Kushlinskii N.E. (2018). Circular RNA: New regulatory molecules. Bull Exp. Biol. Med. 164, 803-815.

Bi R., Wei W., Lu Y., Hu F., Yang X., Zhong Y., Meng L., Wang M., Jiang L. and Xie X. (2020). High hsa_circ_0020123 expression indicates poor progression to non-small cell lung cancer by regulating the miR-495/HOXC9 axis. Aging (Albany NY) 12, 17343-17352.

Braicu C., Zimta A.A., Harangus A., Iurca I., Irimie A., Coza O. and Berindan-Neagoe I. (2019). The function of non-coding RNAs in lung cancer tumorigenesis. Cancers (Basel) 11, 605.

Bray F., Ferlay J., Soerjomataram I., Siegel R.L., Torre L.A. and Jemal A. (2018). Global cancer statistics 2018: GLOBOCAN estimates of incidence and mortality worldwide for 36 cancers in 185 countries. CA Cancer J. Clin. 68, 394-424.

Cai X., Lin L., Zhang Q., Wu W. and Su A. (2020). Bioinformatics analysis of the circRNA-miRNA-mRNA network for non-small cell lung cancer. J. Int. Med. Res. 48, 300060520929167.

Chen L., Nan A., Zhang N., Jia Y., Li X., Ling Y., Dai J., Zhang S., Yang Q., Yi Y. and Jiang Y. (2019). Circular RNA 100146 functions as an oncogene through direct binding to miR-361-3p and miR-615-5p in non-small cell lung cancer. Mol. Cancer. 18, 13.

Chi Y., Luo Q., Song Y., Yang F., Wang Y., Jin M. and Zhang D. (2019). Circular RNA circPIP5K1A promotes non-small cell lung cancer proliferation and metastasis through miR-600/HIF-1alpha regulation. J. Cell Biochem. 120, 19019-19030.

Conchon S., Cao X., Barlowe C. and Pelham HR. (1999). Got1p and Sft2p: membrane proteins involved in traffic to the Golgi complex. EMBO J. 18, 3934-3946.

Consortium E.P., Birney E., Stamatoyannopoulos J.A., Dutta A., Guigo R., Gingeras T.R., Margulies E.H., Weng Z., Snyder M., Dermitzakis E.T., Thurman R.E., Kuehn M.S., Taylor C.M., Neph S., Koch C.M., Asthana S., Malhotra A., Adzhubei I., Greenbaum J.A., Andrews R.M., Flicek P., Boyle P.J., Cao H., Carter N.P., Clelland G.K., Davis S., Day N., Dhami P., Dillon S.C., Dorschner M.O., Fiegler H., Giresi P.G., Goldy J., Hawrylycz M., Haydock A., Humbert R., James K.D., Johnson B.E., Johnson E.M., Frum T.T., Rosenzweig E.R., Karnani N., Lee K., Lefebvre G.C., Navas P.A., Neri F., Parker S.C., Sabo P.J., Sandstrom R., Shafer A., Vetrie D., Weaver M., Wilcox S., Yu M., Collins F.S, Dekker J., Lieb J.D., Tullius T.D., Crawford G.E., Sunyaev S., Noble W.S., Dunham I., Denoeud F., Reymond A., Kapranov P., Rozowsky J., Zheng D., Castelo R., Frankish A., Harrow J., Ghosh S., Sandelin A., Hofacker I.L., Baertsch R., Keefe D., Dike S., Cheng J., Hirsch H.A., Sekinger E.A., Lagarde J, Abril J.F., Shahab A., Flamm C., Fried C., Hackermuller J., Hertel J., Lindemeyer M., Missal K., Tanzer A., Washietl, S, Korbel, J, Emanuelsson, O, Pedersen J.S., Holroyd, N, Taylor R., Swarbreck D., Matthews N., Dickson M.C., Thomas D.J., Weirauch M.T., Gilbert J., Drenkow J., Bell I., Zhao X., Srinivasan K.G., Sung W.K., Ooi H.S., Chiu K.P., Foissac S., Alioto T., Brent M., Pachter L., Tress M.L., Valencia A., Choo S.W., Choo C.Y., Ucla C., Manzano C., Wyss C., Cheung E., Clark T.G., Brown J.B., Ganesh M., Patel S., Tammana H., Chrast J., Henrichsen C.N., Kai C., Kawai J., Nagalakshmi U., Wu J., Lian Z., Lian J., Newburger P., Zhang X., Bickel P., Mattick J.S., Carninci P., Hayashizaki Y., Weissman S., Hubbard T., Myers R.M., Rogers J., Stadler P.F., Lowe T.M., Wei C.L., Ruan Y., Struhl K., Gerstein M., Antonarakis S.E., Fu Y., Green E.D., Karaoz U., Siepel A., Taylor J., Liefer L.A., Wetterstrand K.A., Good P.J., Feingold E.A., Guyer M.S., Cooper G.M., Asimenos G., Dewey C.N., Hou M., Nikolaev S., Montoya-Burgos J.I., Loytynoja A., Whelan S., Pardi F., Massingham T., Huang H., Zhang N.R., Holmes I., Mullikin J.C., Ureta-Vidal A., Paten B., Seringhaus M., Church D., Rosenbloom K., Kent W.J., Stone E.A., Program N.C.S., Baylor College of Medicine Human Genome Sequencing, C, Washington University Genome Sequencing C., Broad I., Children's Hospital Oakland Research I., Batzoglou S., Goldman N., Hardison R.C., Haussler. D., Miller W., Sidow A., Trinklein N.D., Zhang Z.D., Barrera L., Stuart R., King D.C., Ameur A., Enroth S., Bieda M.C., Kim J., Bhinge A.A., Jiang N., Liu J., Yao F., Vega V.B., Lee C.W., Ng P., Shahab A., Yang A., Moqtaderi Z., Zhu Z., Xu X., Squazzo S., Oberley M.J., Inman D., Singer M.A., Richmond T.A., Munn K.J., Rada-Iglesias A., Wallerman O., Komorowski J., Fowler J.C., Couttet P., Bruce A.W., Dovey O.M., Ellis P.D., Langford C.F., Nix D.A., Euskirchen G, Hartman S., Urban A.E., Kraus P., Van Calcar S., Heintzman N., Kim T.H., Wang K., Qu C., Hon G., Luna R., Glass C.K., Rosenfeld M.G., Aldred S.F., Cooper S.J., Halees A., Lin J.M., Shulha H.P., Zhang X., Xu M., Haidar J.N., Yu Y., Ruan Y., Iyer V.R., Green R.D., Wadelius C., Farnham P.J., Ren B., Harte R.A., Hinrichs A.S., Trumbower H., Clawson H., Hillman-Jackson J., Zweig A.S., Smith K., Thakkapallayil A., Barber G., Kuhn R.M., Karolchik D., Armengol L., Bird C.P., de Bakker P.I., Kern A.D., Lopez-Bigas N., Martin J.D., Stranger B.E., Woodroffe A., Davydov E., Dimas A., Eyras E., Hallgrimsdottir I.B., Huppert J., Zody M.C., Abecasis G.R., Estivill X., Bouffard G.G., Guan X., Hansen N.F., Idol J.R., Maduro V.V., Maskeri B., McDowell J.C., Park M., Thomas P.J., Young A.C., Blakesley R.W., Muzny D.M., Sodergren E., Wheeler D.A., Worley K.C., Jiang H., Weinstock G.M., Gibbs R.A., Graves T., Fulton R., Mardis E.R., Wilson R.K., Clamp M., Cuff, J., Gnerre S., Jaffe D.B., Chang J.L., Lindblad-Toh K., Lander E.S., Koriabine M., Nefedov M., Osoegawa K., Yoshinaga Y., Zhu B. and de Jong P.J. (2007). Identification and analysis of functional elements in 1% of the human genome by the ENCODE pilot project. Nature 447, 799-816.

D'Agostino G., Saporito A., Cecchinato V., Silvestri Y., Borgeat A., Anselmi L. and Uguccioni M. (2018). Lidocaine inhibits cytoskeletal remodelling and human breast cancer cell migration. Br J. Anaesth. 121, 962-968.

Du J., Zhang L., Ma H., Wang Y. and Wang P. (2020). Lidocaine suppresses cell proliferation and aerobic glycolysis by regulating circHOMER1/miR-138-5p/HEY1 axis in colorectal cancer. Cancer Manag. Res. 12, 5009-5022.

Evan G.I. and Vousden K.H. (2001). Proliferation, cell cycle and apoptosis in cancer. Nature 411, 342-348.

Feitelson M.A., Arzumanyan A., Kulathinal R.J., Blain S.W., Holcombe R.F., Mahajna J., Marino M., Martinez-Chantar M.L., Nawroth R., Sanchez-Garcia I., Sharma D., Saxena N.K., Singh N., Vlachostergios P.J., Guo S., Honoki K., Fujii H., Georgakilas A.G., Bilsland A., Amedei A., Niccolai E., Amin A., Ashraf S.S., Boosani C.S., Guha G., Ciriolo M.R., Aquilano K., Chen S., Mohammed S. I., Azmi A.S., Bhakta D., Halicka D., Keith W.N. and Nowsheen S. (2015). Sustained proliferation in cancer: Mechanisms and novel therapeutic targets. Semin. Cancer Biol. 35 Suppl. S25-S54.

Guan E., Liu H. and Xu N. (2021). Lidocaine suppresses gastric cancer development through Circ_ANO5/miR-21-5p/LIFR axis. Dig Dis Sci. (in press).

Hansen T.B., Jensen T.I., Clausen B.H., Bramsen J.B., Finsen B., Damgaard C.K. and Kjems J. (2013). Natural RNA circles function as efficient microRNA sponges. Nature 495, 384-388.

Hombach S. and Kretz M. (2016). Non-coding RNAs: Classification, biology and functioning. Adv. Exp. Med. Biol. 937, 3-17.

Ikeda K., Horie-Inoue K., Ueno T., Suzuki T., Sato W., Shigekawa T., Osaki A., Saeki T., Berezikov E., Mano H. and Inoue S. (2015). miR-378a-3p modulates tamoxifen sensitivity in breast cancer MCF-7 cells through targeting GOLT1A. Sci. Rep. 5, 13170.

Jiang G., Wu A.D., Huang C., Gu J., Zhang L., Huang H., Liao X., Li J., Zhang D., Zeng X., Jin H., Huang H. and Huang C. (2016). Isorhapontigenin (ISO) Inhibits invasive bladder cancer formation in vivo and human bladder cancer invasion *in vitro* by targeting STAT1/FOXO1 axis. Cancer Prev. Res. (Phila). 9, 567-580.

Jones G.S. and Baldwin D.R. (2018). Recent advances in the management of lung cancer. Clin. Med. (Lond). 18, s41-s46.

Ko J., Weil A., Maxwell L., Kitao T. and Haydon T. (2007). Plasma concentrations of lidocaine in dogs following lidocaine patch

application. J. Am. Anim. Hosp. Assoc. 43, 280-283.
Kristensen L.S., Andersen M.S., Stagsted L.V.W., Ebbesen K.K., Hansen T.B. and Kjems J. (2019). The biogenesis, biology and characterization of circular RNAs. Nat. Rev. Genet. 20, 675-691.
Lev R. and Rosen P. (1994). Prophylactic lidocaine use preintubation: a review. J. Emerg. Med. 12, 499-506.
Liu H., Dilger J.P. and Lin J. (2020). Effects of local anesthetics on cancer cells. Pharmacol. Ther. 212, 107558.
Ma Q., Huai B., Liu Y., Jia Z. and Zhao Q. (2021). Circular RNA circ_0020123 promotes non-small cell lung cancer progression through miR-384/TRIM44 axis. Cancer Manag. Res. 13, 75-87.
Mitchell S.J, Merry A.F., Frampton C., Davies E., Grieve D., Mills B.P., Webster C.S., Milsom, F.P., Willcox T.W. and Gorman D.F. (2009). Cerebral protection by lidocaine during cardiac operations: a follow-up study. Ann. Thorac. Surg. 87, 820-825.
Ng W.L., Mohd Mohidin T.B. and Shukla K. (2018). Functional role of circular RNAs in cancer development and progression. RNA Biol. 15, 995-1005.
Panda A.C. (2018). Circular RNAs act as miRNA sponges. Adv. Exp. Med. Biol. 1087, 67-79.
Patop I.L. and Kadener S. (2018). circRNAs in cancer. Curr. Opin. Genet. Dev. 48, 121-127.
Piegeler T., Votta-Velis E.G., Liu G., Place A.T., Schwartz D.E., Beck-Schimmer B., Minshall R.D. and Borgeat A. (2012). Antimetastatic potential of amide-linked local anesthetics: inhibition of lung adenocarcinoma cell migration and inflammatory Src signaling independent of sodium channel blockade. Anesthesiology 117, 548-559.
Pleguezuelos-Villa M., Nacher A., Hernandez M.J., Buso M., Barrachina M., Penalver N. and Diez-Sales O. (2019). A novel lidocaine hydrochloride mucoadhesive films for periodontal diseases. J. Mater Sci. Mater Med. 30, 14.
Qu D., Yan B., Xin R. and Ma T. (2018a). A novel circular RNA hsa_circ_0020123 exerts oncogenic properties through suppression of miR-144 in non-small cell lung cancer. Am. J. Cancer Res. 8, 1387-1402.
Qu X., Yang L., Shi Q., Wang X., Wang D. and Wu G. (2018b). Lidocaine inhibits proliferation and induces apoptosis in colorectal cancer cells by upregulating mir-520a-3p and targeting EGFR. Pathol. Res. Pract. 214, 1974-1979.
Siegel R.L., Miller K.D., Fuchs H.E. and Jemal A. (2021). Cancer statistics, 2021. CA Cancer J. Clin. 71, 7-33.
Sisti M.S., Nishida F., Zanuzzi C.N., Laurella S.L., Cantet R.J.C. and Portiansky E.L. (2019). Lidocaine protects neurons of the spinal cord in an excitotoxicity model. Neurosci. Lett. 698, 105-112.
Song H., Li H., Ding X., Li M., Shen H., Li Y., Zhang X. and Xing L. (2020). Long noncoding RNA FEZF1AS1 facilitates nonsmall cell lung cancer progression via the ITGA11/miR516b5p axis. Int. J. Oncol. 57, 1333-1347.
Soto G., Naranjo Gonzalez M and Calero F. (2018). Intravenous lidocaine infusion. Rev. Esp. Anestesiol. Reanim. (Engl Ed). 65, 269-274.
Suhail Y., Cain M.P., Vanaja K., Kurywchak P.A., Levchenko A., Kalluri R. and Kshitiz. (2019). Systems biology of cancer metastasis. Cell Syst. 9, 109-127.
Sun H. and Sun Y. (2019). Lidocaine inhibits proliferation and metastasis of lung cancer cell via regulation of miR-539/EGFR axis. Artif. Cells Nanomed. Biotechnol. 47, 2866-2874.
Thomas L.F. and Saetrom P. (2014). Circular RNAs are depleted of polymorphisms at microRNA binding sites. Bioinformatics 30, 2243-2246.
Wan J., Hao L., Zheng X. and Li Z. (2019). Circular RNA circ_0020123 promotes non-small cell lung cancer progression by acting as a ceRNA for miR-488-3p to regulate ADAM9 expression. Biochem. Biophys. Res. Commun. 515, 303-309.
Wang C., Tan S., Li J., Liu. W.R., Peng Y. and Li W. (2020a). CircRNAs in lung cancer - Biogenesis, function and clinical implication. Cancer Lett. 492, 106-115.
Wang L., Zhao L. and Wang Y. (2020b). Circular RNA circ_0020123 promotes non-small cell lung cancer progression by sponging miR-590-5p to regulate THBS2. Cancer Cell Int. 20, 387.
Wen J., Li X., Ding Y., Zheng S. and Xiao Y. (2021). Lidocaine inhibits glioma cell proliferation, migration and invasion by modulating the circEZH2/miR-181b-5p pathway. Neuroreport 32, 52-60.
Xu T., Song X., Wang Y., Fu S. and Han P. (2020). Genome-wide analysis of the expression of circular RNA full-length transcripts and construction of the circRNA-miRNA-mRNA network in cervical cancer. Front Cell Dev. Biol. 8, 603516.
Yang Y., Wu J., Zhou H., Liu W., Wang J. and Zhang Q. (2020). STAT1-induced upregulation of lncRNA LINC01123 predicts poor prognosis and promotes the progression of endometrial cancer through miR-516b/KIF4A. Cell Cycle 19, 1502-1516.
Zeeshan R. and Mutahir Z. (2017). Cancer metastasis - tricks of the trade. Bosn J. Basic Med. Sci. 17, 172-182.
Zhang L., Hu R., Cheng Y., Wu X., Xi S., Sun Y. and Jiang H. (2017). Lidocaine inhibits the proliferation of lung cancer by regulating the expression of GOLT1A. Cell Prolif. 50, e12364.
Zhang L., Cheng A., Yu Y., Zou N., Wang W., Lv L., Guo X., Chen M. and Zhang Y. (2020). GOLT1A-KISS1 fusion is associated with metastasis in adenoid cystic carcinomas. Biochem. Biophys. Res. Commun. 526, 70-77.
Zhao Y., Wang Y. and Xing G. (2018). miR-516b functions as a tumor suppressor by directly modulating CCNG1 expression in esophageal squamous cell carcinoma. Biomed. Pharmacother. 106, 1650-1660.
Zhao L., Ma N., Liu G., Mao N., Chen F. and Li J. (2021). Lidocaine Inhibits Hepatocellular Carcinoma Development by Modulating circ_ITCH/miR-421/CPEB3 Axis. Dig. Dis. Sci. 66, 4384-4397.
Zhu J., Zhang Y., Yang X. and Jin L. (2017). Clinical significance and tumor-suppressive function of miR-516b in nonsmall cell lung cancer. Cancer Biother. Radiopharm. 32, 115-123.

Accepted January 21, 2022